Examining the influence of winglets on the blade geometry of tiny horizontal-axis wind turbines is an area that has seen a lot of experimental study recently.

CHINTA SEKHAR 1, P NAVEEN REDDY 2,
ASSOCIATE PROFESSOR 1, ASSISTANT PROFESSOR 2,
Mail ID:sekharresonance1975@gmail.com, Mail Mail ID:naveena0346@gmail.com
Dept.: Mechanical
Nagole Institute of Technology and Science,
Kuntloor(V),Hayathnagar(M),Hyderabad,R.R.Dist.-501505.

ABSTRACT

This study aims to examine and improve the performance of a tiny horizontal axis wind turbine blade operating at low wind speeds. The experimental blades were created utilizing an additive manufacturing method including 3D printing. At wind speeds between 2 and 6 meters per second, we examined air foils including the E210, NACA2412, S1223, SG6043, E216, NACA4415, SD7080, SD7033, S1210, and MAF. At a Reynolds number of 100,000, Foil was used to study the air foils and determine the ideal blade shape. Tip speed ratios between 3 and 10 were examined, along with solidities between 0.0431-0.1181 and angles of attack between 2 and 20 degrees. To optimize and further investigate the power coefficient, lift coefficient, drag coefficient, and lift to drag ratio, these variables were later adjusted in the MATLAB and Foil software. The rotors' cut-in wind speed was 2 and 2.5 m/s with and without winglets, respectively. Air foils with optimal geometries for the given operating circumstances and production process outperformed their NACA 2412, S1223, SD7080, S1210, and SD7003 counterparts. These included the E210, SG6043, E216, NACA4415, and MAF.

Keywords:

Keywords: air foils, aerodynamic efficiency, power coefficient, rigidity, tip speed ratio.

INTRODUCTION

Horizontal-axis wind turbines (HAWTs) and vertical-axis wind turbines (VAWTs) are the two main types of wind generators (HAWT). Generally speaking, VAWTs can produce greater power at a lower wind speed than HAWTs. As a result, VAWTs are more cost-effective for usage in neighbourhoods. At the same wind speed, however, HAWT is predicted to create greater power due to reduced aerodynamic drag and increased wind power generated by the spinning of all blades (Lee et al., 2016). Most SWTs are built to operate in a broad range of wind speeds without the ability to adjust their pitch. Given their intended function, it is preferable that SWTs have air foils that are effective at low Reynolds numbers, can start up and generate energy at relatively low wind speeds, and need little in the way of maintenance. Additionally, SWTs should be accessible to the common person in terms of price, dependability, and lack of maintenance. As a result, there is often a compromise to be made between maximizing performance and keeping the design and operation as simple as possible (Ismail et al., 2018). One needs at least 4.2 m/s of wind speed for a tiny wind turbine with a horizontal axis to function. The improved blade may be used to lower the beginning speed without the need for external effort, opening up the possibility of deployment in roadside or rooftop settings (Abrar et al., 2014).

Another study looked at the first-use performance of tiny rotors and found that the majority of the torque-generating power came from the blade tips (Wright and Wood, 2004; Clifton and Wood, 2007). The Blade element momentum (BEM) model was shown to provide the highest accuracy and the most computing efficiency in calculating propeller performance after being compared to other blade element models (Gur and Rosen, 2008). Subsonic flow was studied in two dimensions over a NACA 0012 and SG6043 air foil at a Reynolds number of 3 x 106 in a different study (Patel et al., 2014 and Chaudhary & Prakash 2019). The distribution of chord and twist angles of tiny wind turbine blades was also researched to determine the optimal values for maximizing the yearly energy output of such devices.

METHODS AND MATERIALS

The BEM technique is widely used as a viable option for designing wind turbines. This theory proposes that Blade Element Theory and Momentum Theory may be used to determine the axial and tangential forces operating on the turbine blade. For a wind turbine, a power coefficient of 0.593 is the highest possible value. The Betz limit refers to this upper bound. In this research, we utilized Foil to create a new kind of air foil and

improve the profile of wind turbine blades with and without winglets.

Method of Calculation

Fig. 1 shows a schematic of the Foil method for optimizing air foils and designing the geometry of rotor blades. Fig. 2 depicts the rotor experiment's blade geometry. In this research, BEMT is utilized for Foil simulation-based aerodynamic design and optimization of a rotor blade for a tiny wind turbine at low Reynolds number.

When calculating the aerodynamic performance of a wind turbine, Eq. (1) [11] shows that the Reynolds number (Re) of the air foil has a significant impact.

$$Re = \frac{\rho V c}{\mu}$$

1

Here, V is the speed of the wind (in meters per second), c is the chord length of the air foil (in meters), and is the dynamic viscosity of the fluid (in Newton-meters per squared centimeters). Using Eq. (1), we can determine how much the air foil's Solidity () impacts the wind turbine's aerodynamic performance (2)

$$\sigma = \frac{B \times C}{\pi R^2}$$

2

where B is the blade count, C is the blade area in square meters, and R is the blade's diameter (m). From Eq. (3- 4), we can get the values for Torque (T) and turbine output power (P):

$$T = \frac{P}{\omega}$$

$$P = VI$$

3 & 4

where denotes the angular velocity in radians per second, N represents the rotor speed in revolutions per minute as measured by a laser tachometer, and I represent the rotor's supply

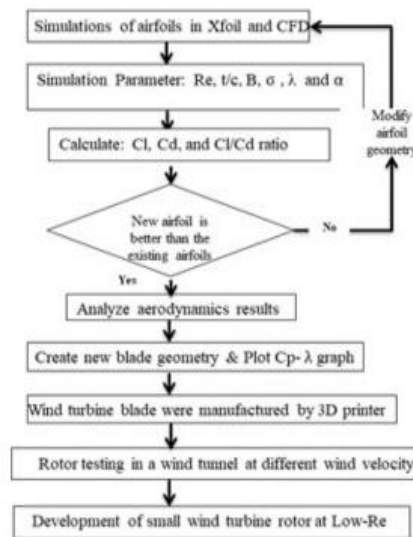voltage and current. The voltmeter measures V and I at varying wind speeds.

Figure 1 An overview of the Foil process for creating air foils and rotor blades.

AN INTERACTIVE APPROACH

Optimization of the Blade Geometry with and without a Rotor Winglet

Various rotor geometries are shown in Fig. 2. For this research, the PLA-made blade of a tiny wind turbine was used since it had the best theoretical efficiency for a rotor at a TSR of 4-7. Using the modified air foil, the rotor blades' radii were 0.2 m with and without the winglet. New air foil B = 3 with and without winglet rotors, showing how chord and twist angle change with sectional blade length at different rotors (R1, R2, R3, and R4). It was estimated that the winglet angle was 70 degrees, and that the winglet height ranged from 1.5 to 2.0 cm in chord. In the case of the winglet R2 rotor, the maximum and minimum chords were 0.026 m and 0.018 m, respectively, for a twist angle of 14.89° at the root and 1.29° at the tip; in the case of the winglet R4 rotor, the corresponding values were 0.047 m and 0.032 m, respectively, for a twist angle of 23.17° at the root and 3.98 m, respectively. Figure 4 shows the optimal blade shape for quick prototype fabrications, with Solidity = 4.31-11.81%. Chord length and twist angle were found to decrease with

increasing blade length. Since increasing the twist angle raises the cost and complexity of manufacture, a cap of 40 degrees was decided upon. The blade geometry of the R2 rotor was shaped like a winglet, but the R1, R3, and R4 rotors did not have any such features. Rotor R1 has a solidity of 0.043, rotor R2 of 0.06, rotor R3 of 0.0726, and rotor R4 of 0.1181.
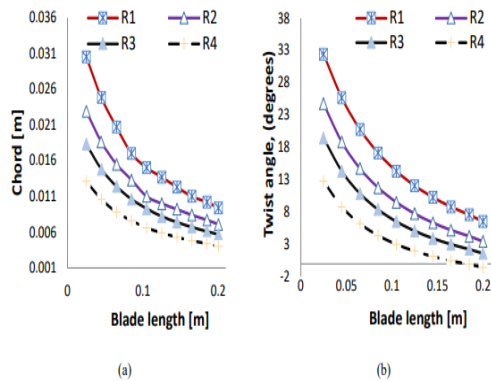

Figure 2. Specifically, the geometry of the blade. Blade length vs chord size (a). (b) The ratio of the blade's twist to its length.

Manufacturing a Rotor Blade for a Miniature Wind Turbine 3D printing (Additive manufacturing)

using PLA filaments was used to create the blade geometry for the miniature wind turbines shown in Fig. 2. With the help of the Cure program, we were able to export the Creo files as G code and load them into the 3D printer. The printer was operated with the following settings: nozzle temperature of 205 degrees Celsius, bed temperature of 60 degrees Celsius, and printing resolution of 0.001 meters. Blade analysis and test stands for the four different models of wind turbines utilized in the experiment are shown in Figure 3. A 7-blade blower fan powered by a 5.59 kw electric motor spinning at 1500 rpm and excited by a 200 V DC supply was used to adjust the air velocity between 3 and 30 m/s. A 0.3 m 0.3 m 1 m test segment is available in the tunnel. The wind speeds that the HTC anemometer could detect ranged from 1 to 30 meters per second. The features of the Model 560 digital tachometer are as follows: The HTM-560 has the following specifications: working temperature of 0 to 60 °C, measuring

distance of 0.075 to 0.3 m, resolution range of 0.1 to 1000 rpm, basic accuracy of 0.05% reading +1 digit, and 0 to 60 °C. Fig. 4 depicts the experimental setup.
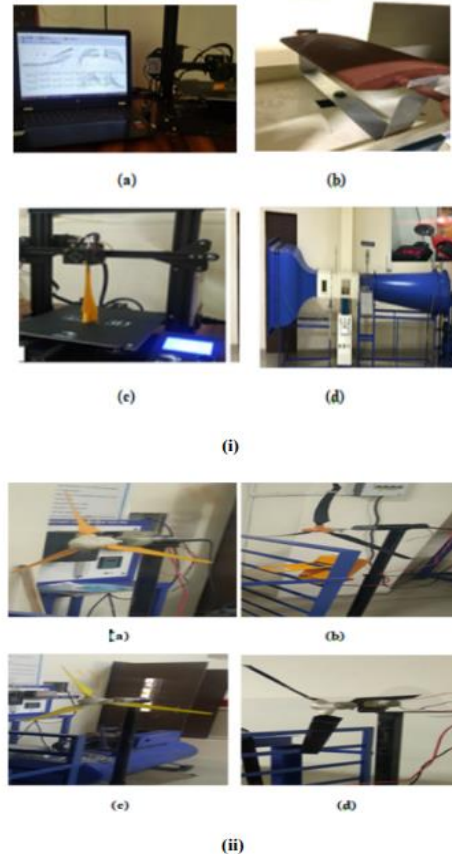

Figure 3: Analysis and construction of a blade. I Air foilmodelling using the Foil program. An Updated Air foil (wooden material). (c) 3D-printed blade production (PLA material). The d) experimental test rig. [ii] variable-density 3D-printed rotors for wind turbines: In order: (a) R1; (b) R2; (c) R3; (d) R4.
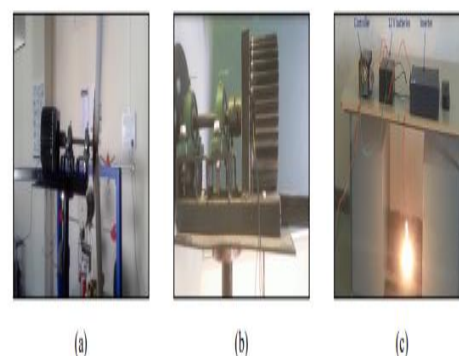
Figure 4. Experimental setup: (a) shaft coupling arrangement; (b) alternator; (f) inverter.

RESULTS AND DISCUSSION

In this part, we report the findings from our numerical and experimental analyses of all of the examples. An experimental study was conducted on a 3-blade wind turbine rotor with wind velocities ranging from cut-in speed (2 m/s) to rated wind speed (6 m/s) and rotor solidities ranging from 4.31 percent to 11.811 percent. Table 2 lists the highest values of the power coefficient of rotor for a variety of air foils and solidities at a Reynolds number of 100,000.

Analysis of Other Air foils and Their Potential Use in the Design of Blades for Small Wind Turbines

Figures 5 and 6 show a comparison of the MAF air foil's aerodynamic performance to that of the E210, NACA2412, S1223, SG6043, E216, NACA4415, SD7080, SD7003, and S1210 air foils in the Foil findings (a-b). Lift and lift-to-drag ratio graphs for the 10 air foils at Re=100,000 are shown in Figs. 5 (a-b). The tests were conducted utilizing Foil. Figure 5(a) shows that the angle of attack () has a significant effect on the lift coefficient values. The results graph shows that the S1223 air foil has the greatest lift coefficient values between 2 and 12 degrees of angle of attack, while the mixed air foil (MAF) air foil comes in second. The graph shows that the greatest CL for the S1223 and the MAF air foil occur at an angle of attack, of 12o. At an angle of 14 degrees, the CL of an S1210 air foil reaches its maximum value of 1.8. For the S1123 and MAF air foil, the value of CL falls after 12o angle of attack down to angle of attack, =16o; the value of CL stays constant up to 20o angle of attack at CL =1.8. Maximum CL for the air foils S1210, E216, E210, and NACA4415 is 1.83, 1.5, 1.32, and 1.32 respectively at an angle of attack, of 12 degrees. Comparatively, the maximum CL=1.18 was achieved by the SD7003 and SD7080 at an angle of attack of 12 degrees, while the highest CL=1.51 was achieved by the SG6043 air foil at an angle of attack of 14 degrees. In the angle of attack range of 12-16o, the air foils MAF, S1210, E216, NACA4415, and SG6043 exhibited soft stall behaviour. At a low Reynolds number =100,000, Fig. 5(b) displays the range of lift-to-drag ratios (CL/CD) for various air foils. With an incidence angle () of 4o, the E216 air foil generated the highest lift-to-drag ratio (CL/CD) of 67.35, followed by the S1210 and SG6043 air foils at s of 66.16 and 66.16, respectively. At = 6o, the highest CL/CD values for air foils MAF, S1223, E210,

SD7080, NACA4415, NACA2412, and SD7003 are 62.22, 58.13, 56.4, 51.7, 51.7, 48.88, and 45.06. At an angle of attack of 2 degrees, the SD7003 and NACA2412 air foils have CL/CD ratios of 33.2 and 34.48, respectively. Finally, it was determined from the Foil results that the E216, SG6043, NACA2412, E210, and S1223 air foils produced their maximum lift-to-drag ratios at a specific value, while the MAF, S1210, SD7080, NACA44515, and NACA4415 air foils produced a broad range of CL/CD ratios and exhibited a soft stall behaviour in the angle of attack.
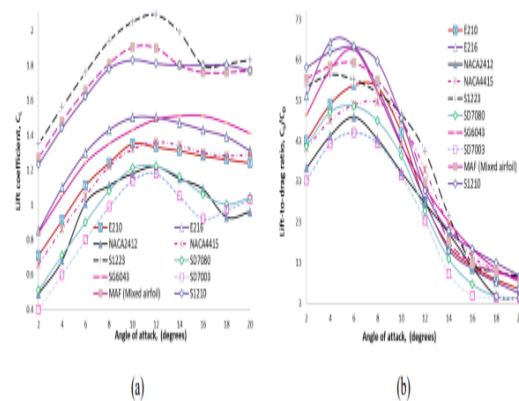

Figure 5. Variations of (a) lift coefficient (CL), (b) lift-to-drag ratios (CL/CD) of different air foils at Reynolds number = 100,000.

Small horizontal axis wind turbines operating at low Reynolds numbers were found to benefit from the MAF air foil's profile. At an angle of attack (AOA) between 5 and 6 degrees and a Reynolds number (Re) of 100,000, the CL/CD ratio for the investigated air foil reached its highest value.

Power Coefficient as a Function of Air foil and Tip Speed Ratio at a Value of 0.0431

Specifically, the BEMT-based design software was developed for tip speed ratios between 2 and 8. Cp-was plotted using Foil. Several low-Re air foils with blade numbers ranging from 3 to 9 were evaluated for their solidities at Re=100,000, with the findings shown in Fig. 6. The solidities ranged from 4.31 percent to 11.81 percent, with the blade geometry being twisted and the chord changing (a–d). Figure 6(a) shows that for rotor R1 with solidity = 4.31%, the Cp values rise with a maximum tip speed ratio of up to 7, and subsequently drop for all other air foils except for air foils S1223 and S1210. Air foils E210, E216, SG6043, NACA2412, NACA4415, SD7080, SD7003, and MAF have maximum Cp = 0.43, 0.46, 0.38, 0.42, 0.39, 0.37, and 0.44 at = 7, as shown in Figure 6(a), whereas

air foils S1223 and S1210 have maximum Cp = 0.45 and 0.46. The investigation showed that for small horizontal axis wind turbines, Solidity = 4.31% was the sweet spot for the E216, SG6043, NACA4415, and MAF (New Air foil) profiles.

Power Coefficient as a Function of Air foil and Tip Speed at an Angular Velocity of = 0.0604
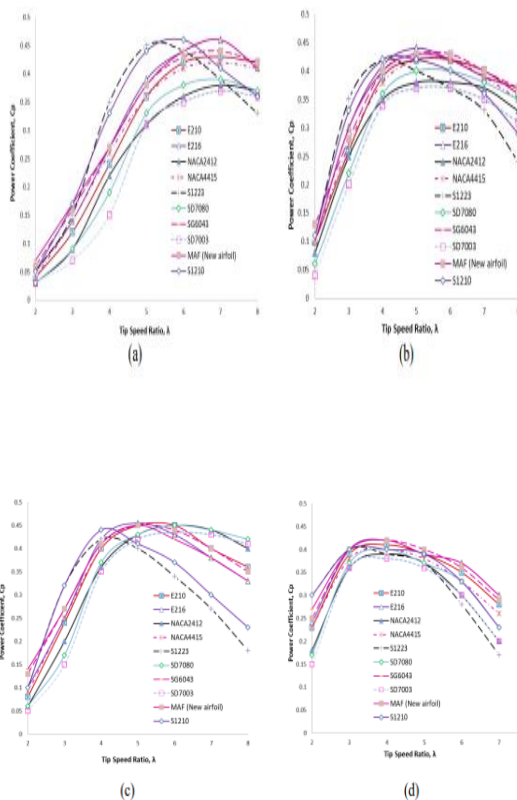

Figure 6: The relationship between the power coefficient and the tip speed ratio for three distinct rotor air foils at a rotational speed of Re=100,000 (R4).

At solidity = 6.04%, the power coefficient of the various rotor R2 air foils with winglet blade shape are shown in Fig. 6(b). Cp = 0.42, 0.38, 0.43, 0.44, 0.42, 0.4, 0.37, and 0.43 at = 5 for the BEMT-R2 rotor's air foils E210, NACA 2412, SG6043, E216, NACA4415, SD7080, SD7003, and MAF, and Cp = 0.42 and 0.42 for the S1223 and S1210 air foils at top speed ratios = 4, respectively. Finally, the BEMT-R2 rotor's E210, SG6043, E216, NACA4415, and MAF air foils were found to be the best ideal for wind turbine blades thanks to their broad tip speed ratio, = 4 to 6 at Solidity = 6.04%.

Power Coefficient as a Function of Air foil and Tip Speed Ratio for = 0.0726

Figure 6(c) displays the power coefficient of rotor R3 of various air foils without winglet blade shape at Solidity = 7.26 percent. From Fig.6 (c), we can see that the maximum Cp for an R3 rotor is 0.45 for air foils E210, SG6043, E216, NACA4415, and MAF at = 5, 0.45 for air foils NACA2412, SD7080, and SD7003, and 0.435 for air foils S1223 and S1210, all at a tip speed ratio of = 4. The numerical calculations concluded that the BEMT-R3 rotor, which includes the NACA2412, SD7080, SD7003, and MAF, was the most suitable for wind turbine blades because of its broad tip speed ratio, = 4 to 7 at solidity = 7.26%.

Changes in Power Efficiency Due to Air foil Aspect Ratio and Tip Speed at = 0.1181

At solidity = 11.81 percent, without the winglet blade shape shown in Fig. 6 (d), the power coefficient of several air foils of rotor R4 is shown. Maximum Cp = 0.4, 0.41 and 0.39, 0.42, 0.42, 0.4, 0.4, 0.4, 0.38, and 0.42 are shown for R4 rotor air foils E210, NACA2412, S1223, SG6043, E216, NACA4415, SD7080, SD7003, S1210, and MAF in Fig. 6(d). Final results from the numerical calculations showed that the BEMT-R3 rotor, which includes materials like E216, SG6043, and MAF, is most suited for wind turbine blades thanks to its broad range of tip speed ratio, = 3 to 5 at solidity = 11.81%. Finally, the Cp- graph suggested that the MAF air foil, BEMT-blade, was chosen for small wind turbines because to its broad range of tip speed ratios, from 4-7 for a solidity, ranging of 4.31% to 11.81%.

3D Printing Performance Evaluation Using MAF Air foil for Resolutions R1, R2, R3, and R4

Using a blade pitch angle of 22 degrees, Fig. 7 displays the experimental findings of the fluctuation in wind speed (a-b). Figure 7(a) shows that when the turbine rotor solidity increases, the torque values increase as well. However, the torque generated by the R2 and R3 rotors with and winglet blade shape is almost the same up to the rated wind speed, the maximum torque produced by the R3-rotor. According to visual depictions, the winglet geometry blade generates more torque than the rotor without a winglet, although using less power. Equations 3 and 4 may be used to determine torque and power at different wind speeds. Power production from changeable rotors for changing wind speeds is shown in Figure 7(b). When comparing the R3, R2, and R1 rotors, the R3 rotor produces the most power between 2.5 and 6 meters per second. The results graph shows that the

winglet rotor R2 has the second-highest output power in the 2-6 m/s wind speed range, behind the rotor R4. The R2 rotor with the winglet generates higher power in the 5-6 m/s wind speed range than the R2 rotor without the winglet at about the same solidity. Between 80% and 85% of errors were passed on to the next level of processing. Approximate findings from Foil were 20%-30% off from those from experiments. The values found using Foil were greater than those found in experiments.
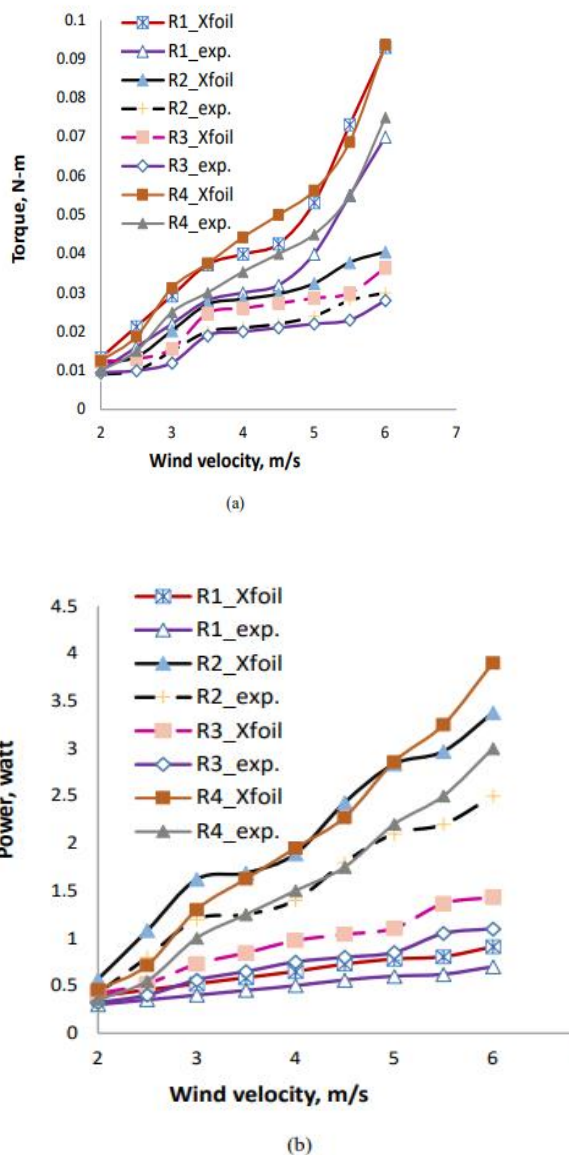

(a)

(b)

Figure 7. (a) Torque distribution of the R1, R2, R3, and R4 rotors with new air foil blade section. (b) Power distributions of the R1, R2, R3, and R4 rotors at different wind speed.

CONCLUSIONS

It is hypothesized in this research that a new kind of air foil may function effectively at low Reynolds numbers. Existing low Reynolds number air foils (E210, NACA2412, S1223, SG6043, E216, NACA4415, SD7080, SD7033, and S1210) were used to improve the MAF air foil using Xfoil. This research looks at 10 different low Reynolds number air foils with a Reynolds number of 100,000. The largest soft behaviour range of the MAF, S1210, and SG6043 air foils made them the best candidates for compact horizontal axis wind turbines at low Reynolds number. Maximum Air foil Area (MAF) was shown to be the air foil best suited to provide maximum power at low Re values, both in computational and experimental studies. Four BEMT-based test models with 3-blades and 0.2 m blade radius were built using additive manufacturing using PLA material. The design and production of the four rotors with a solidity of 0.0431-0.1181 was completed. Only the R2 rotor was fitted with winglets, whereas the other three (R1, R3, and R4) were constructed with the same MAF air foil cross section but without winglets. Blade element momentum theory was used to optimize the blade geometry of all 10 air foils with respect to tip and root losses (BEMT). With respect to the tip speed ratio (), we experimented with different values for the power coefficient (Cp) of the newly designed and chosen air foils (MAF). The simulation results show that at = 7, the MAF air foil blade has an optimal power coefficient of Cp = 0.44, for Reynolds number (Re) = 100,000 and solidity (S) = 0.0431 without a winglet. The highest power coefficient for the MAF air foil blade is 0.43 at = 5, and 0.45 at Re = 100,000, with a solidity of 0.0604 and 0.0726, respectively. At = 4, solidity = 0.1181, the power coefficient was around 0.42. Therefore, the numerical simulation concluded that the MAF air foil was the best air foil for delivering maximum power in low-wind conditions. It's official when: 0 0.5 1 1.5 2 2.5 3 3.5 4 4.5 2 3 4 5 6 7 intensities, in watts Number of meters per second that the wind is blowing First, we have R1 Xfoil and R1 exp, then R2 Xfoil and R2 exp, R3 Xfoil and R3 exp, and finally R4 Xfoil and R4 exp. That rotor performance is maximized with winglet blade geometry at solidities below 10%, whereas high rotor efficiency is generated without winglet blade geometry at solidities between 7% and 12%. The rotors' improved starting performance is the result of the greater solidity's ability to provide a high torque at a relatively low tip speed ratio (4.5–5). When the blade's solidity is less than 12%, the performance of the rotor and the tip speed ratio are directly affected by the air foil's shape. Theoretical and practical findings imply that the R4 and R2 rotors'

shape is better suited for low-wind-speed use on compact horizontal-axis wind turbines.

REFERENCES

[1] Abrar, M. A., Mahbub, A. M. & Mamun, M. 2014. Design Optimization of a Horizontal Axis Micro Wind Turbine through Development of CFD Model and Experimentation,10th International Conference on Mechanical Engineering Procedia, Engineering, 90: 333-338. C

[2] Chaudhary, M K, and Prakash, S. 2019. Investigation of Blade Geometry and Air foil for Small Wind Turbine Blade, American Scientific Publishers 11(5): 448-452.

[3] Clifton-Smith, M.J. & Wood, D. H. 2007. Further dual-purpose evolutionary optimization of small wind turbine blades, J. Phys. Conf. Ser., 75: 012017 Gur, O. & Rosen, A. 2008. Comparison between blade-element models of propellers. Aeronaut J.112:689–704

[4] Hassan Zadeh, A., Hassan Abad, H.H. & Dadvand, A. 2016. Aerodynamic shape optimization and analysis of small wind turbine blades employing the Viterna approach for post-stall region, Alexandria Engineering Journal. 55 (3): 2035-2043.

[5] Ismail, A.R.K., Thiago, Canali. & Fatima, A.M. Lino. 2018. Parametric analysis of Jankowskiair foil for10- kW horizontal axis windmill, Journal of the Brazilian Society of Mech. Sciences and Engineering. 40, Article no: 179.

[6] Khaled, M., Ibrahim, M. M., Hamed, A. H., and Ahmed, F. 2019. Investigation of a small Horizontal Axis wind turbine performance with and without winglet, Energy, 187:115921.

[7] Lee, M.H., Shieh, Y.C. & Chi Jang, B. 2016. Experiments and numerical simulations of the rotor- blade performance for a small-scale horizontal axis wind turbine, J. Wind Eng. Ind. Aerodynamics.149: 17 – 29.

[8] Nataraja, M., and Balaji, G. 2019, Study on performance of wind mill by adding winglet in turbine blade: Virtual analysis, Journal of scientific & industrial research,78 :96-101. Patel, K. S., Pate, S. B., Patel, U. B., and Ahuja, A. P., 2014,

[9] "CFD Analysis of an Aerofoil" International Journal of Engineering Research, 3: 154 – 158. Suresh, A. &Rajkumar, S. 2019. Design of small horizontal axis wind turbine for low wind speed rural application, Material today proceeding.23 (1):16-22

[10] Saravanan, P., Paramania, K., and Rajang, S. 2013. Experimental Investigation on Small Horizontal Axis Wind Turbine Rotor Using Winglet, Journal of Applied Science and Engineering, 16 (2):159-164.

[11] Wright, A.K. & Wood, D.H. 2004. The starting and low wind speed behaviour of a small horizontal axis wind turbine, Journal of Wind Engineering and Industrial Aerodynamics. 92:1265-1279.